

THE TRANSFERABILITY OF MICRO-MECHANICAL DAMAGE PARAMETERS IN MODERN LINE PIPE STEEL

S. H. Hashemi, I. C. Howard, J. R. Yates and R. M. Andrews*

The University of Sheffield, Department of Mechanical Engineering, Sheffield, UK

*Advantica Technologies Ltd, Loughborough, UK

s.h.hashemi@shef.ac.uk

Summary

The Charpy upper shelf energy is widely used to assess the toughness requirements of gas pipeline steels. It has been suggested that the Charpy energy associated with crack propagation can be split in two parts. One is related to flat fracture at the centre of a typical Charpy fracture surface and the other corresponds to slant fracture at the edges. As the dominant failure mechanism in gas pipelines is fast propagating ductile shear, the latter is the most important portion of the fracture energy which can be reasonably attributed to the real failure mode of the pipe. Proper specimens with different flat and slant fracture characteristics are needed for a comprehensive failure analysis of the Charpy specimen.

This paper describes recent results from an experimental and computational set of studies on high-toughness gas pipeline steel of grade API X100. The test matrix consisted of three sets of specimens with different fracture characteristics. It included standard C(T) specimens and tensile bars, a novel slant C(T) specimen and a modified double cantilever beam (DCB), and Charpy V-notch specimens. Each specimen type was associated with studies of flat, slant and mixed mode fracture, respectively.

An attempt to use the Gurson ductile damage model to cross-correlate all the experimental data was qualitatively successful in general and was also quantitatively reliable for fracture dominated by flat tearing. However it was not quite accurate enough to transfer the slant C(T) data to the modified DCB test. Despite that, the insight obtained suggested that an energy transfer model is relevant, and the paper concludes by showing how this can be used to apportion the data from the Charpy test.

Introduction

Design against ductile fracture for low-grade pipeline steels has traditionally focused on the concept of overall absorbed fracture energy from Charpy or drop weight tear test (DWTT) specimen. However, the application of upper shelf Charpy energy to assess pipeline tearing resistance can result in significant errors when the pipe toughness is increased [1]. This indicates that semi-empirical formulae calibrated in past on test data from less tough steels cannot be extrapolated to assess the fracture toughness of modern pipeline steels. A main source of the discrepancy is that the Charpy energy in high-strength high-toughness pipeline materials is dominated by failure processes other than slant fracture. For instance, the high initiation energy occupies a considerable portion of the overall fracture energy in high grade API X80 and X100 pipeline steels [2].

It has been suggested by e.g. Leis [3] and Andrews et al. [4] that the fracture energy in Charpy impact test associated with fracture propagation can be split in two parts. One is related to flat

fracture at the centre of the typical Charpy fracture surface and the other to slant fracture at the edges. As the dominant failure mechanism in gas line pipes is fast propagating ductile shear, the latter is the most important portion of the fracture energy which can be reasonably attributed to the real failure mode of the pipe. Accordingly, proper specimens with different flat and slant fracture characteristics are needed for a comprehensive failure analysis of the Charpy specimen.

The paper reports recent results using the modified Gurson model [5-6] for ductile fracture in an attempt to transfer data extracted from Charpy and other tests to assess the behaviour of specimen types that are more directly relevant to the behaviour of ductile tearing of gas pipelines. The model was tuned on appropriate plain and notched tensile bars for the flat fracture characteristics. Validation of this model was achieved by reproducing the experimental C(T) data.

The paper describes similar techniques to transfer data between slant fracture specimens. It goes on to assess the performance the Charpy impact behaviour of X100 steel through the use of a three-dimensional finite element model, and concludes by apportioning the energy absorbed in various processes in the Charpy test in a way that can extract data directly applicable to running ductile tears in gas pipelines.

Material properties

The material under investigation was an API X100 grade gas pipe (36" O.D×19mm W.T). The chemical composition of the steel is set out in Table 1.

TABLE 1. Chemical composition of X100 steel reported by pipe manufacturer

element	C	Si	Mn	P	S	Cu	Ni	Cr	Mo	Nb	Ti	Al
(wt%)	0.06	0.18	1.84	0.008	0.001	0.31	0.5	0.03	0.25	0.05	0.018	0.036

To measure the pipe tensile properties, a plate was taken from the 180° position (where the seam weld was located at 0°) of the original pipe and machined to 15.8mm thickness. Four round tensile bars having a 40mm gauge length and 10mm gauge diameter were extracted in the pipe circumferential direction as shown in Fig. 1.

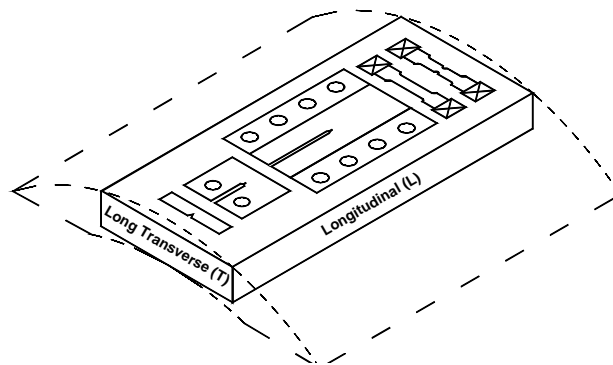


FIGURE 1. Orientation of test specimens in the original pipe

All tensile experiments were performed on a servo-hydraulic Instron 8501 test machine under displacement control of 0.01mm/s. Table 2 contains the measured mechanical properties of X100 steel.

Table 2. X100 steel mechanical properties in transverse direction

Young's modulus GPa	Yield strength (0.2% proof stress) MPa	Tensile strength MPa	Yield/UTS
210	769	823	0.93

Experimental work on flat and slant fracture

Smooth round tensile bars and standard compact tension C(T) specimens were tested at a low strain rate to record the load-displacement data for tuning the finite element damage model for flat fracture. The two sets of laboratory specimens with different geometry and constraint levels provided sufficient data of ductile flat fracture characteristics of X100 steel.

In the tensile tests, a transverse extensometer was used to capture the reduction of specimen diameter during the test. The load-diametral contraction was measured from three sets of tensile specimens having different gauge diameter and notch acuity. From the plain bar specimens, true stress-strain data required for finite element computation was obtained.

A clip-gauge was used on the C(T) specimens to monitor the crack mouth opening displacement (CMOD). All test samples were sidegrooved up to 20% of the specimen original thickness according to ASTM E1820 [7] to reduce the shear lip formation near the side surfaces of the specimens.

Shear fracture experiments were conducted on two sets of specimens. A novel slant C(T) and a modified double cantilever beam [8] were used for this purpose. Photographs of both specimens are shown in Fig. 2.



FIGURE 2. Photograph of slant notch C(T) (left) and modified DCB (right) after the test

All shear specimens were taken from the same plate in the TL orientation (where T is the transverse and the L is the longitudinal directions), see Fig. 1. The maximum available thickness with respect to the pipe curvature was 15.8mm. Slant C(T) specimens of 10 and 12mm thicknesses were tested on a Schenck 250kN machine whereas tear testing on DCB specimen was conducted on an ESH 1000kN test machine. DCB specimens had gauge thickness of 8, 10 and 12mm. In each experiment the load, load line displacement and CMOD were recorded. The load-CMOD data were subsequently used for tuning the FE model.

Gurson damage model for ductile fracture

The simulation of all test specimens was carried out using the modified Gurson ductile damage theory. The Gurson model is typically expressed in the form of the yield potential:

$$\Phi = \left(\frac{\sigma_{eq}}{\sigma_Y}\right)^2 + 2q_1 f \cosh\left(-q_2 \frac{3p}{2\sigma_Y}\right) - (1 + q_3 f^2) = 0 \quad (1)$$

where σ_{eq} is the von Mises equivalent stress, σ_Y the material yield strength, p the hydrostatic pressure, q_1 , q_2 and q_3 are material constants, and f is the damage parameter. The values of the q parameters are typically around $q_1=1.5$, $q_2=1.0$ and $q_3=q_1^2$ for ferritic steels.

In this model fracture propagates when the damage parameter reaches its critical value designated by f_c (threshold of rapid loss of stress carrying capacity). The damaged elements are removed from the analysis simulating crack growth through the microstructure. The final void volume fraction at total failure is represented by f_f . These two, as well as the parameters q_1 and q_2 , are supposed to be material constants. Therefore, in total, four constants should be determined to perform the damage simulation.

The initial void volume fraction can be calculated from the Franklin's formula [10]:

$$f_o = f_v \frac{(d_x d_y)^{1/2}}{d_z} \quad (2)$$

$$f_v = 0.054 \left(S\% - \frac{0.001}{Mn\%} \right) \quad (3)$$

where d_x , d_y and d_z are the average dimensions of the inclusions. If a spherical inclusion shape is assumed, equation (2) gives $f_o = f_v$. From this an initial void volume fraction $f_o = 3 \times 10^{-5}$ was found for this steel.

Flat and slant fracture modelling

The finite element code ABAQUS 6.2 was used throughout the analyses [9]. Due to symmetry, only one quarter of the tensile bars and C(T) specimens were modelled. Axi-symmetric elements were used for the tensile specimens whereas the C(T) specimens were simulated by 2D plane strain elements. To tune the damage model parameters for flat fracture, the experimental data from tensile bars and C(T) specimens was used. Typical values of the q parameters were input in the FE routine to start the simulation. The critical and final void volume fraction as well as the cell size were determined by a trial and error procedure until the model response matched the experimental data.

A plot of the test data and the tuned model for notch bar tensile specimens of 8mm gauge diameter and 6mm notch radius, typical of X100 steel is shown in Fig. 3. The slight difference between the test and simulation response at the final stage of the experiment was due to shear band formation at the specimen edges which led to a rapid failure.

The tuned damage parameters on tensile specimens ($q_1=1.5$ and $q_2=1.05$) were transferable to C(T) specimens. The comparison of load-CMOD data from the test and computation for a C(T) specimen is shown in Fig. 3.

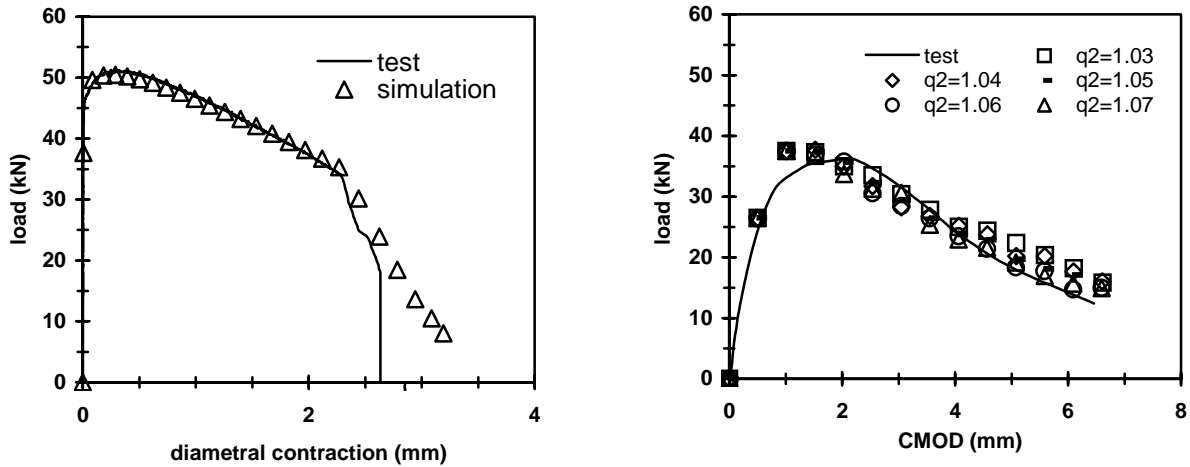


FIGURE 3. FE simulation of notch tensile bar (left) and C(T) specimen (right)

Similarly, the tuning of the failure model for shear fracture was conducted using the test data from slant C(T) and DCB specimens. 2D elements were used to construct the plane strain FE model. Typical values of the q parameters were used to start the simulation in FE model of the slant C(T) specimen. The same critical void volume fraction ($f_o = 3 \times 10^{-5}$), the first damage parameter $q_1 = 1.5$ and the critical mesh size ($l_c = 200 \mu m$) were applicable in shear fracture modelling whereas a slightly different value for q_2 was required to simulate the tests.

Fig. 4 illustrates the results for the slant C(T) specimen. The model response was sensitive to the variation of the q_2 damage parameter and a value of $q_2 = 0.98$ was able to simulate the experiment. As can be seen, apart from the early stage of the test, the model response agrees well with the experiment record.

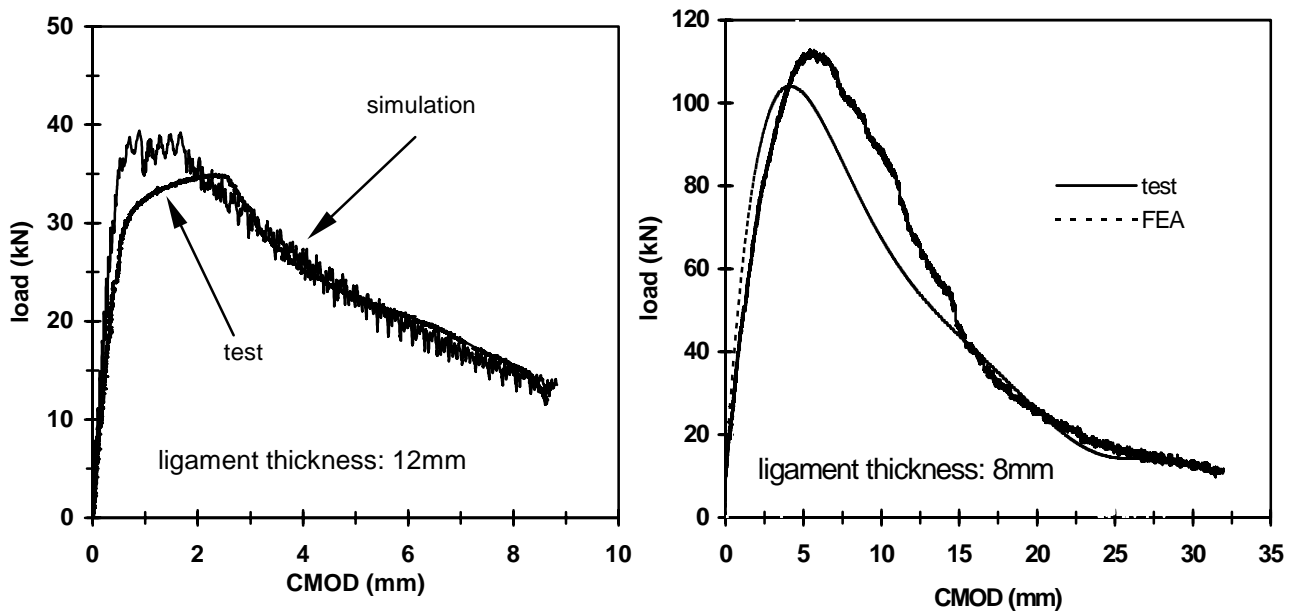


FIGURE 4. FE simulation of slant C(T) specimen (left) and DCB (right)

When the same value of q_2 as was tuned on the slant C(T) test was used to predict the fracture behaviour of DCB specimens, a rather rapid failure of the specimen resulted. A lower q_2 value, of the order of 0.75, was needed to approximately simulate the tear specimens, see Fig. 4. Since the experimental tear test of Fig. 4 only displayed fully-developed shear fracture after the CMOD has reached about 15mm, one might regard the accuracy of fit of the data when the CMOD is greater than 15mm as evidence of successful data transfer. (The comparatively poor agreement in the records before the CMOD=15mm is almost certainly due to the influence of flat fracture modes in the tearing process). Unfortunately, this agreement is only available through the use of a different q_2 from that used to represent the tearing in the slant C(T) specimen. Despite this, the partial agreement exhibited in Fig. 4 is strong evidence for the existence of an underlying mechanics of data transfer, strongly modulated by the influence of flat fracture modes and of three-dimensional effects. Further evidence for this view comes from the work of Seshadri et. al. [11] which reports the combination of two stress states in a 2D shear fracture simulation of thin C(T) and M(T) aerospace aluminium alloy specimens through the application of a plane strain core near the crack tip and plane stress conditions elsewhere. Although this requires the use of the 3D FEA for determining the height of the plane strain core, it better represents the actual stress state in the test samples.

Simulation of Charpy impact test

Further insight into the fracture processes of the mixed mode flat and slant failure was sought through the use of a full 3D dynamic analysis of a Charpy impact specimen. Due to symmetry, only one quarter of the specimen was simulated. The striker and the anvil were modelled as elastic bodies. Contact conditions were applied between the striker and specimen and between the anvil and specimen. An initial hammer velocity of 5.5m/s was applied in impact orientation. Fig. 5 shows the results.

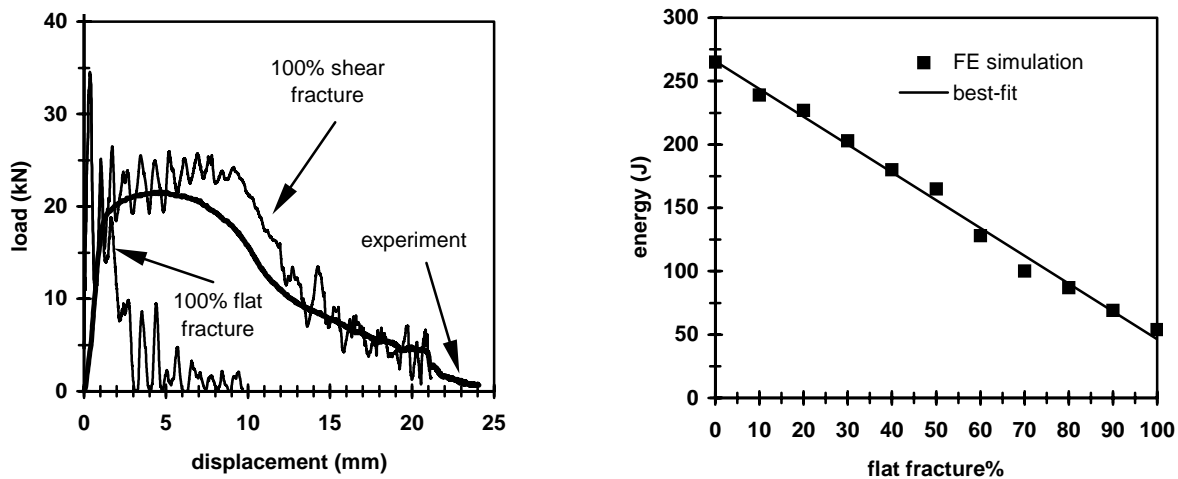


FIGURE 5. Simulation of Charpy experiment using $q_1 = 1.05$ and $q_2 = 0.60$ (left) and Charpy energy as a function of flat fracture percentage (right)

The model response varied as q_2 changed with a tendency towards a better agreement between the test and simulation for smaller values of q_2 . Values of the order of 0.60 to 0.65 for the second damage parameter were able to numerically simulate the impact experiments. Using

this as the slant failure criterion for X100 steel together with the previously calibrated parameters on flat tearing, models were constructed with different proportions of slant and flat fracture. The extreme cases of 100% flat and 100% slant are most informative and are discussed here.

The variation so obtained of the total fracture energy as a function of the percentage of flat fracture on the fracture surface of the Charpy specimen is shown in Fig. 5. The plot indicated that the absorbed energy dropped linearly as the flat fracture percentage increased with a minimum of 54J for 100% flat fracture model. The 100% slant fracture model gave the maximum impact energy of 260J. This latter value was within 5% of the experimental result.

Close inspection of the simulation showed that initiation of cracking occurred near the peak load and 84J of energy had been consumed. This was in good agreement with 83J energy consumed up to the peak load in the experiment. A further 73J of energy was consumed in non-fracture processes such as indentation and bending, leaving 103J consumed in shear propagation. The corresponding energies for the 100% flat fracture model were 2J at initiation, 19J in non-fracture deformation and 33J in flat tearing.

It is evident that in high strength, high toughness steels the Charpy energy from a test is dominated by non-crack propagation energies. Around 40% (103/260) of the measured energy appeared to be associated with shear fracture which is the important mechanism in linepipe tearing.

An energy balance for the Charpy test can be accomplished as follows. The energy per area unit in flat fracture specimens (1.1 J/mm^2) was measured from the standard C(T) specimens. Similarly, the slant fracture energy per area unit (1.6 J/mm^2) was derived from the stable phase of crack propagation of the DCB specimens. Flat crack growth is less energy-demanding (up to 30%) than slant crack propagation which requires larger fracture surfaces. This is consistent with the energy drop in Fig. 5 as the flat fracture area increases on the fracture surface of Charpy specimen.

Visual inspection of the surface of the broken Charpy specimens showed that the percentage of flat and slant fracture areas was around 60% and 40%, respectively. This is equivalent to 53J flat and 72J slant fracture energy. Although this slant fracture energy is 30% less than the FE estimation, the values indicate that most of the energy in Charpy specimens made from modern tough pipeline steels is consumed in non-shear fracture processes. The energy due to shear cracking evaluated by either test or FE model could be as low as 30% and 40% of the total fracture energy. This implies the application of correction factors of 2.5-3 into the existing propagation/arrest models. Although these values might be conservative, they are comparable with the suggested correction factors of 2 by Leis [3] and 1.7 by Demofonti [12] for predicting the ductile tearing resistance of X100 steel from the Battelle two-curve model. The difference is probably because a proportion of the non-fracture energy should be associated with the shear fracture to obtain an “equivalent” Charpy energy for comparison with the empirically calibrated models. The existing predictive models have all been calibrated using the total energy, where the non-fracture processes are included in the calibration. Further work is in progress to investigate these issues, but the present results support the use of damage mechanics modelling to provide a quantitative understanding of the Charpy test and the derivation of correction factors for the existing models of ductile crack propagation and arrest.

Conclusions

Ductile damage models of flat fracture tests on X100 linepipe steel have been constructed and calibrated using the experimental data from round tensile bars and compact C(T) specimens.

The calibration of damage model parameters on shear fracture have been conducted on a novel slant C(T) and a modified DCB specimen. The tuned micro-mechanical ductile damage parameters have been used in a dynamic 3D numerical simulation of the Charpy impact test. The model has enabled the relative contributions of the deformation and fracture mechanisms to the overall Charpy fracture energy to be estimated. The work suggests that only 30-40% of the impact energy is associated with shear crack propagation in the Charpy test and the rest of the absorbed energy is consumed in flat fracture and non-related fracture processes such as indentation and gross deformation of the test specimen.

Acknowledgements

Support from BP Exploration and Production is Gratefully acknowledged, together with the permission to publish this work. S H Hashemi appreciates helpful discussion with Dr. A Shterenlikht during the experimental work.

References

1. Killmore, C. R., Barbaro, F. J., Williams, J. G. and Rothwell, A. B., In *Proceedings of the International Seminar on Fracture control in Gas Pipelines*, Sydney, Australia, 1997, 4.1-4.19.
2. Pussegoda, N., Malik, L., Dinovitzer, A., Graville, B. A., and Rothwell, A. B., In *Proceedings of the 2000 International Pipeline Conference*, Calgary, Alberta, Canada, Vol. **1**, 2000, 239-245.
3. Leis, B. N., Eiber, R. J., Carlson, L. and Gilroy-Scott, A., In *Proceedings of International Pipeline Conference*, Vol. **II**, ASME, 1998, 723-731.
4. Andrews, R. M., Howard, I. C., Shterenlikht, A. and Yates, J. R., In *Proceedings of the 14th Biennial Conference on Fracture*, ECF14, edited by Neimitz, A. et al., EMAS Publication, Sheffield, 2002, 65-72.
5. Gurson, A.L., *Journal of Engineering Materials and Technology*, Vol. **99**, 1977, 2-15.
6. Tvergaard, V., *International Journal of Fracture Mechanics*, Vol. **17**, 1981, 389-407.
7. ASTM: Standard Test Method for Measurement of Fracture Toughness, E1820-01, American Society for Testing and Materials, West Consohocken, Pennsylvania, 2001.
8. Shterenlikht, A., Hashemi, S. H., Howard, I. C., Yates, J. R. and Andrews, R. M., *Engineering Fracture. Mechanics*, Vol. **71**, 2004, 1997-2013.
9. Hibbitt, H. D., Karlsson, B. I. and Sorensen, E. P., ABAQUS User's Manual (version 6.2), 2001.
10. Franklin, A. G., *J. Iron and Steel Inst.*, **207**, 1969, 181-186.
11. Seshadri, B. R., Newman Jr., J. C. and Dawicke, D. S. *Engineering Fracture Mechanics*, Vol. **70**, 2003, 509 –524.
12. Demofonti, G., Mannucci, G., Harris, D., Barsanti, L. and Hillenbrand, H-G: In: *High Grade Linepipes in Hostile Eenvironments*, November 2002, Yokohama, Edited by R Denys and M Toyoda, Beaconsfield, Scientific Surveys, 2002, 245-261.